

Proceedings of the Fifth Annual LHCP
LHCb-PROC-2017-037
October 14, 2017

New results on heavy-flavour in heavy-ion collisions with LHCb

JIAJIA QIN

*On behalf of the LHCb Experiment,
School of Physical Sciences
University of Chinese Academy of Sciences, Beijing, 100049, China*

ABSTRACT

Heavy-flavour quarks are important to probe Quark-Gluon Plasma(QGP) properties. Cold Nuclear Matter(CNM) effects can be accessed by p Pb collisions.

LHCb is a heavy-flavour precision experiment and has collected large collision data samples. Production cross-section measurements of prompt D^0 at $\sqrt{s_{NN}}=5$ TeV and J/ψ at $\sqrt{s_{NN}}=8.16$ TeV are presented.

PRESENTED AT

The Fifth Annual Conference
on Large Hadron Collider Physics
Shanghai Jiao Tong University, Shanghai, China
May 15-20, 2017

1 Introduction

In nucleus-nucleus collisions, a deconfined thermodynamic system, the so-called Quark-Gluon Plasma(QGP), is expected to be formed. Heavy-flavour quarks are sensitive to measure the properties of the medium since they are produced at an early stage of the collision and, consequently, interact with the created deconfined system. To fully understand the information on the thermodynamic system provided by heavy-quark observables, effects that are not related to the creation of a deconfined system need be well studied. They can be studied with p Pb collisions.

Production cross-section measurements of prompt D^0 at $\sqrt{s_{NN}}=5$ TeV [1] and J/ψ [2] at $\sqrt{s_{NN}}=8.16$ TeV in p Pb collisions are reported in these proceedings. The experimental data is confronted with different types of phenomenological calculations. The nuclear modification of the parton distribution function(PDF) [3] are extracted based on nuclear collision data under the assumption of collinear factorisation. They show modifications of the parton distribution function compared to the one of the free proton and neutron. At low longitudinal momentum fractions x carried by the parton, collinear factorisation may break down and the effective field theory, the so-called Color Glass Condensate(CGC) [4], may provide the more appropriate description of the nucleus as a dense gluonic system. In the Coherent energy loss [5] model, it was proposed that the dominant nuclear modification in quarkonium production might be small angle gluon radiation of the incident quark pair taking properly into account the interference of gluon radiation prior and after the hard-scattering.

2 LHCb detector

LHCb detector [6, 7] is a single-armed detector covering the pseudorapidity range $2.0 < \eta < 5.0$. Due to different beam energies per nucleon for the proton and ^{208}Pb beams, the LHCb detector covers two different acceptance regions in the nucleon-nucleon rest frame: the $1.5 < y^* < 4.5$ corresponding to the “forward” region and $-5.0 < y^* < -2.5$ corresponding to the “backward” region. The rapidity y^* is defined with respect to the direction of the proton beam.

3 Prompt D^0 production in proton-lead collisions at 5 TeV

The decay $D^0 \rightarrow K^\pm \pi^\mp$ is used to reconstruct the signals in the proton-lead data samples collected in 2013. The data sample corresponds to an integrated luminosity of 1.06 ± 0.02 nb $^{-1}$ for the forward region and 0.52 ± 0.01 nb $^{-1}$ for the backward region.

3.1 The single-differential cross-sections

The single-differential cross-sections shown in Fig. 1, are compared with calculations(HELAC-Onia) [10, 11, 12] validated with results of heavy-flavour production cross-section in pp collisions. The results show that the predictions based on EPS09 LO [8], EPS09 NLO [8], nCTEQ15 [9] can give descriptions consistent with data within large theoretical uncertainties. While the nCTEQ15 underestimates data in the low p_T region. The authors of nCTEQ15 pointed out themselves [9] that the gluon distributions are hardly constrained by any data and that, hence, the nPDF uncertainties are albeit their already large size still systematically underestimated.

3.2 Nuclear modification factors

The nuclear modification factor is defined as:

$$R_{p\text{Pb}}(y^*(p_T), \sqrt{s_{NN}}) = \frac{1}{A} \frac{\frac{d\sigma_{p\text{Pb}}}{dy^*(dp_T)}(y^*(p_T), \sqrt{s_{NN}})}{\frac{d\sigma_{pp}}{dy^*(dp_T)}(y^*(p_T), \sqrt{s_{NN}})}, \quad (1)$$

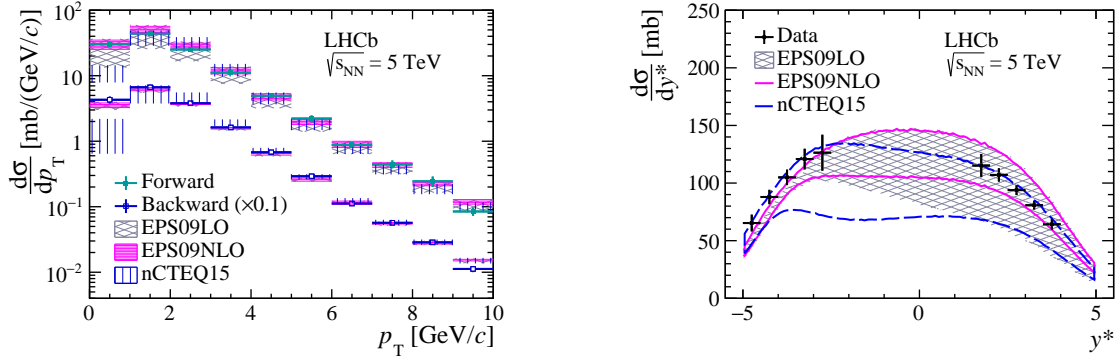


Figure 1: Single-differential cross-section of prompt D^0 meson production in p Pb collisions (left) as a function of p_T and (right) as a function of y^* both in the forward and backward collision samples.

where $A=208$ is the atomic mass number of the lead nucleus. The results integrated over y^* or integrated over p_T both in the forward region and the backward region are shown in Fig. 2. The results are compared with HELAC-Onia calculations using EPS09LO, EPSNLO and nCTEQ15 nPDFs [10, 11, 12]. Calculations based on CGC model [15] are also shown in Fig. 2.

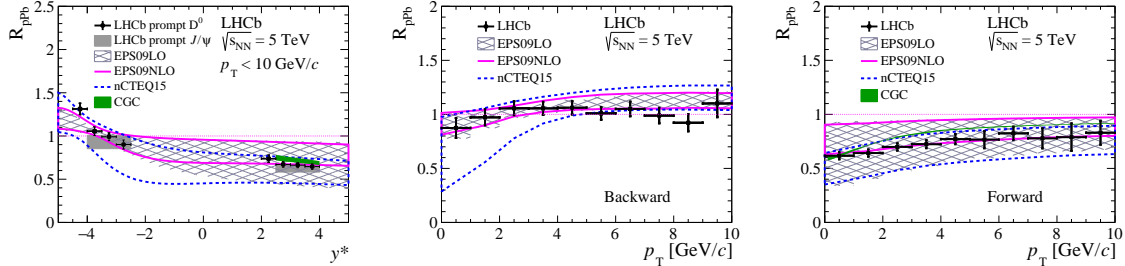


Figure 2: Nuclear modification factor R_{pPb} for prompt D^0 meson production as a function of y^* (left) integrated up to $p_T = 10$ GeV/c and as a function of p_T (middle and right) integrated over the common rapidity range $2.5 < |y^*| < 4.0$ for $p_T < 6$ GeV/c and over $2.5 < |y^*| < 3.5$ for $6 < p_T < 10$ GeV/c.

For R_{pPb} as a function of y^* , there is a strong suppression in the forward region, a nuclear modification factor above unity in the backward region. For the results in the backward region, all three predictions show reasonable agreement with each other and with LHCb data. In the forward region, the HELAC calculations using nCTEQ15 and EPS09LO nPDFs show a better agreement with the data than the calculation with EPS09NLO. The CGC model is found to be able to describe the trend of prompt D^0 meson nuclear modifications as a function of p_T and of rapidity. The nuclear modification factors for prompt D^0 are also compared with those for prompt J/ψ in the left plot of Fig. 2 as a function of rapidity integrated over p_T , and they are found to be consistent.

3.3 Forward-Backward production ratio

The forward-backward production ratio R_{FB} is defined as:

$$R_{FB}(y^*(p_T)) \equiv R_{pPb}(+|y^*|(p_T))/R_{pPb}(-|y^*|(p_T)). \quad (2)$$

In this quantity, a large fraction of the systematic uncertainties cancel. The results are shown in Fig. 3. The ratio of R_{FB} for prompt J/ψ divided by R_{FB} for prompt D^0 mesons is shown in Fig. 4.

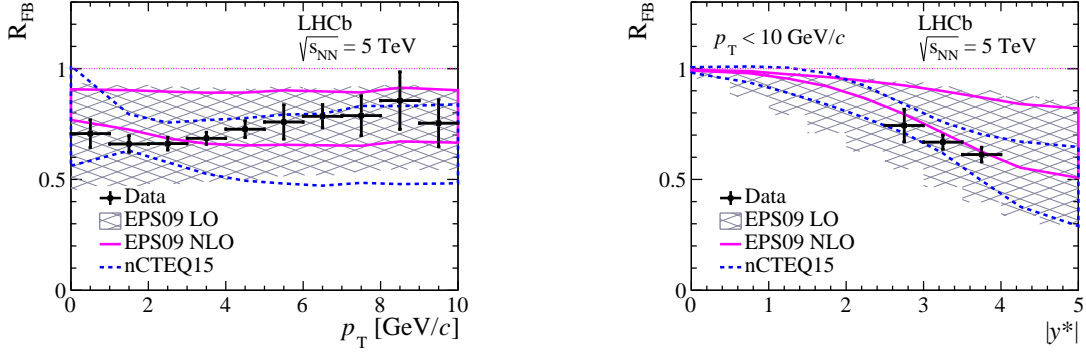


Figure 3: Forward-backward ratio R_{FB} for prompt D^0 meson production as a function of p_{T} (left) integrated over the common rapidity range $2.5 < |y^*| < 4.0$ for $p_{\text{T}} < 6$ GeV/c and over $2.5 < |y^*| < 3.5$ for $6 < p_{\text{T}} < 10$ GeV/c; as a function of y^* (right) integrated up to $p_{\text{T}} = 10$ GeV/c.

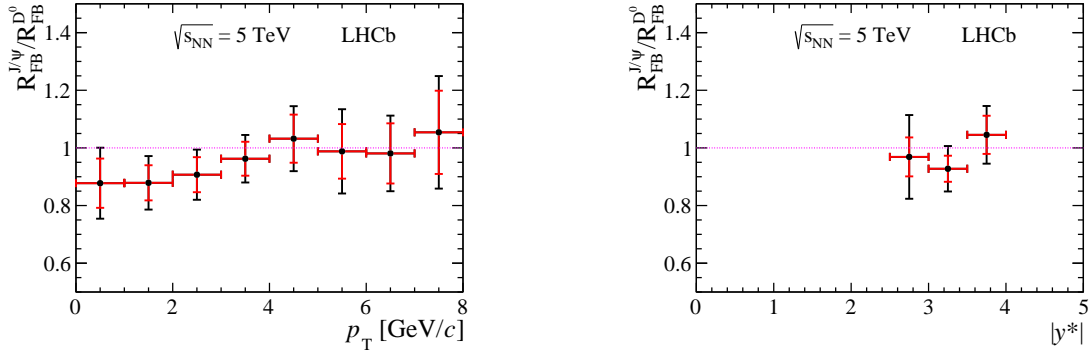


Figure 4: The ratio of the forward-backward ratio with respect to prompt J/ψ as a function of p_{T} (left) and as a function of y^* (right).

Good agreement is found between measurements and HELAC-Onia predictions using EPS09LO [8] and nCTEQ15 [9] nPDFs. The forward-backward production ratio increases slightly with increasing p_{T} and decreases strongly with increasing rapidity $|y^*|$. The measurement shows that R_{FB} has the same size for prompt D^0 and prompt J/ψ mesons within the uncertainties in the LHCb kinematic range.

4 J/ψ production in proton-lead collisions at 8.16 TeV

The production of J/ψ meson was studied in $p\text{Pb}$ collisions at the centre-of-mass energy per nucleon pair $\sqrt{s_{\text{NN}}} = 8.16$ TeV. Prompt J/ψ and nonprompt J/ψ are separated with the pseudo-proper decay time t_z . This measurements are based on the proton-lead collision data samples collected in 2016. The integrated luminosity corresponds to 13.6 ± 0.3 nb $^{-1}$ for the forward region and 20.8 ± 0.5 nb $^{-1}$ for the backward region.

4.1 Single-differential cross-sections

The single-differential cross-sections are compared with the ones from the inter/extrapolated pp reference cross sections [17]. The results are shown in Fig. 5 and Fig. 6. There are some differences especially in the forward region and the low p_{T} region, which highlight the effect of the nuclear environment.

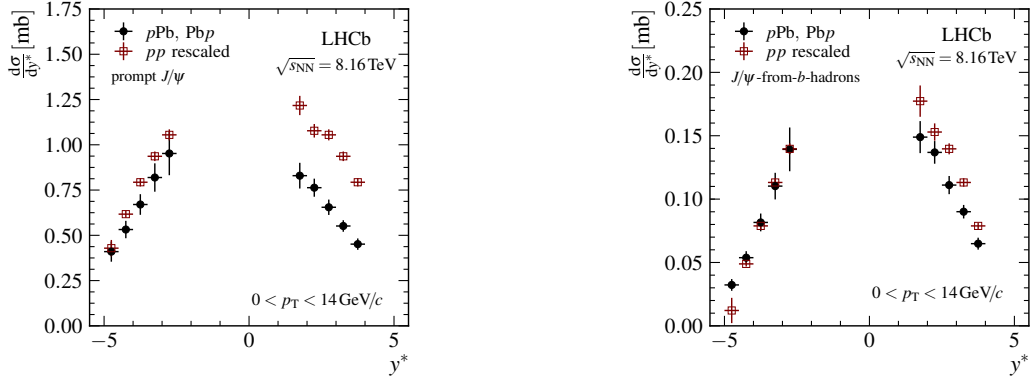


Figure 5: Absolute production cross-sections of (left) prompt J/ψ and (right) J/ψ -from- b -hadrons, as a function of y^* , integrated over the range $0 < p_T < 14 \text{ GeV}/c$.

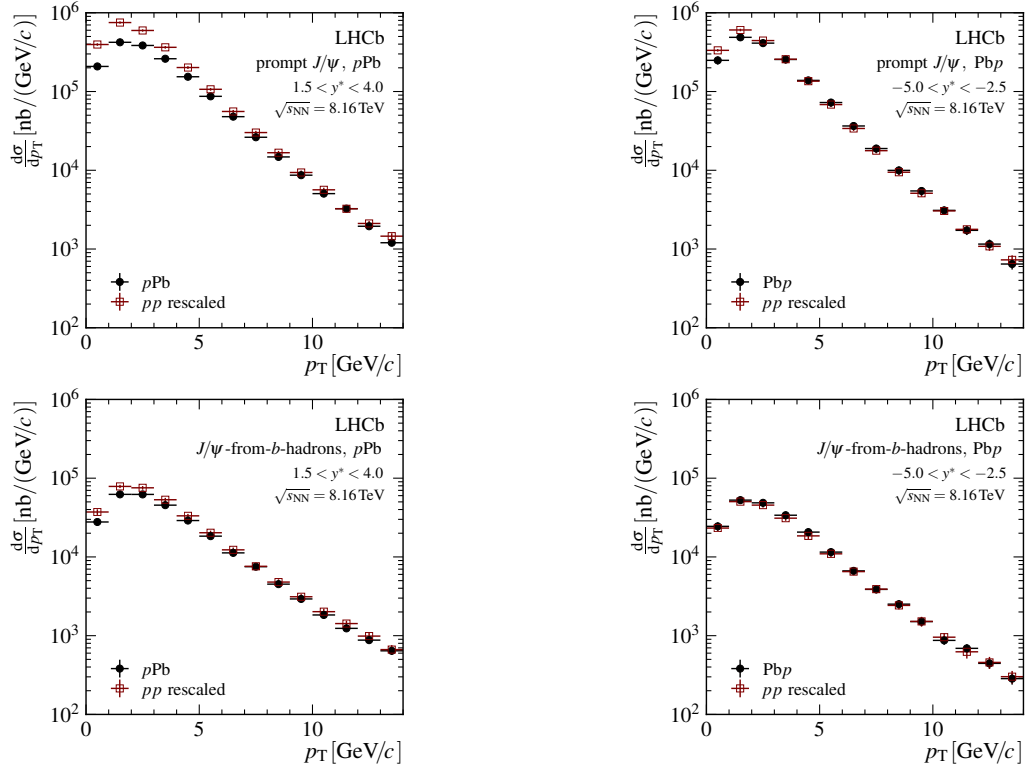


Figure 6: Absolute production cross-sections of (top left) prompt J/ψ in $p\text{Pb}$, (top right) prompt J/ψ in $\text{Pb}p$, (bottom left) J/ψ -from- b -hadrons in $p\text{Pb}$ and (bottom right) J/ψ -from- b -hadrons in $\text{Pb}p$, as a function of p_T and integrated over the rapidity range of the analysis.

4.2 Nuclear modification factors

The nuclear modification factors for prompt J/ψ and nonprompt J/ψ are shown in Fig. 7 and Fig. 8.

At forward rapidity, $1.5 < y^* < 4.0$, a strong suppression of up to 50% is observed in the case of prompt J/ψ at low transverse momentum. With increasing p_T , $R_{p\text{Pb}}$ approaches unity and the suppression is stronger at more forward rapidities. The production of J/ψ -from- b -hadrons is also suppressed compared to that in pp collisions. No dependence as a function of rapidity is observed within the experimental uncertainties.

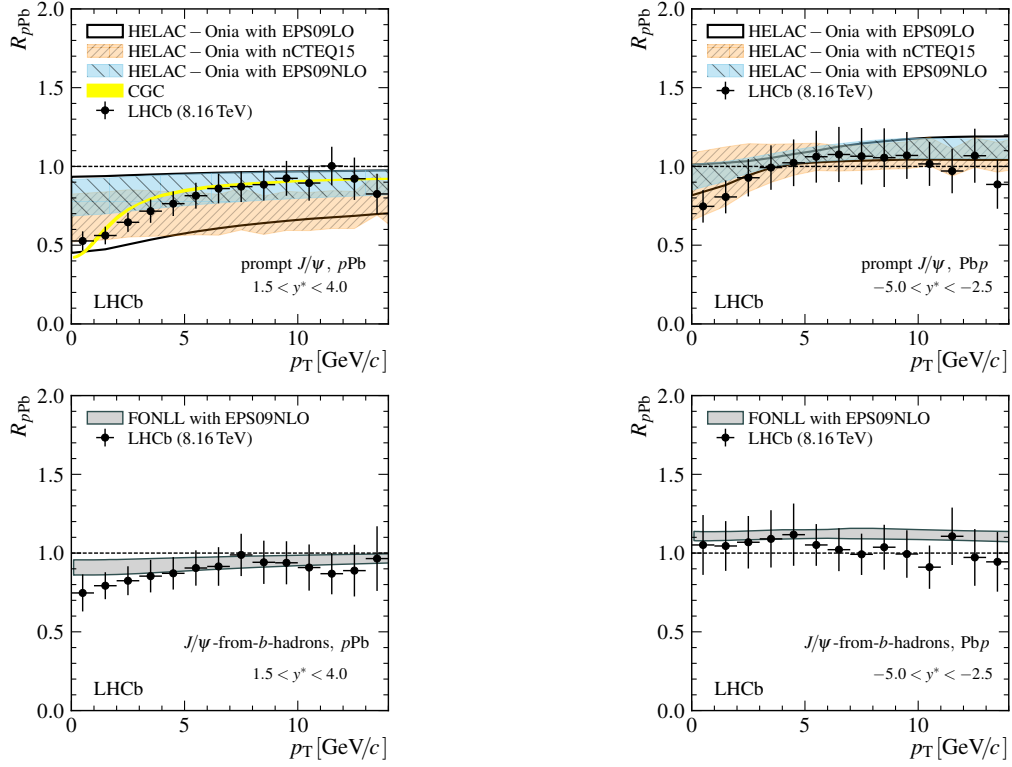


Figure 7: J/ψ nuclear modification factor, R_{pPb} , integrated over y^* in the analysis range, as a function of p_T for (top left) prompt J/ψ in pPb , (bottom left) J/ψ -from- b -hadrons in pPb , (top right) prompt J/ψ in PbP and (bottom right) J/ψ -from- b -hadrons in PbP .

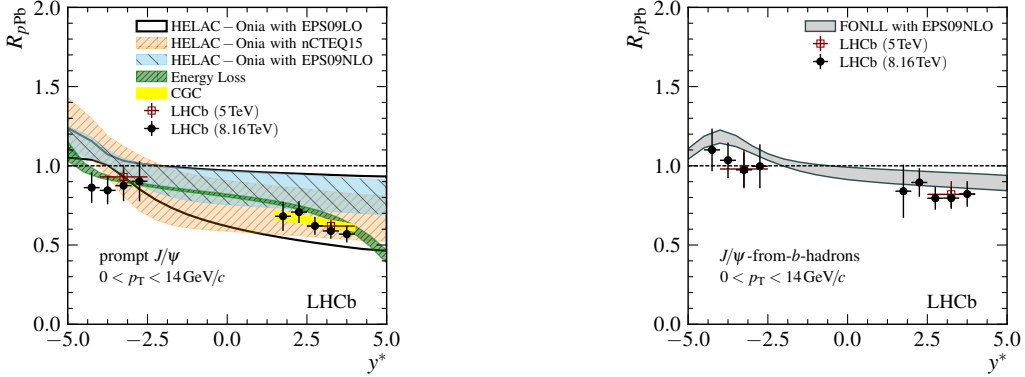


Figure 8: J/ψ nuclear modification factor, R_{pPb} , integrated over p_T as a function of y^* for (left) prompt J/ψ and (right) J/ψ -from- b -hadrons.

The dependence as a function of the transverse momentum is weaker for J/ψ -from- b -hadrons compared to prompt J/ψ .

At backward rapidity, $-5.0 < y^* < -2.5$, a weaker suppression of prompt J/ψ production at low transverse momentum is observed, of up to 25%. Similarly to the forward rapidity region, the suppression is weakening and the nuclear modification factor is approaching values consistent with unity at high transverse momentum.

For the prompt J/ψ results, they are compared with calculations of different groups: collinear factorisation using different nPDFs [11, 12], CGC effective field theory [15, 16] and coherent energy loss [5]. The CGC predictions agree with the behaviour of the data well at forward rapidity and this is the same conclusion in the prompt D^0 measurement. The HELAC-Onia calculations have been tuned to reproduce prompt J/ψ cross-section measurements in pp collision and then combined with different sets of nPDFs. The large uncertainties caused by the missing experimental constraints on the gluon density in the nucleus at low x . At backward rapidities, the experimental points exhibit a different rapidity shape to the calculations and it's different with the shape of the prompt D^0 shown in Fig. 2 as well. The coherent energy loss model is able to provide the overall shape of the suppression, but overestimates the experimental data at forward rapidities.

For the J/ψ -from- b -hadrons results, a perturbative QCD calculation at fixed-order next-to-leading logarithms(FONLL) [13, 14] coupled with the EPS09 nPDF set at next-to-leading order are compared with the data. The measurements overall agree with the calculation within uncertainties. However, the calculation tends to show larger nuclear modification factors than the data and the slope of the theoretical curve is not seen in the experimental data at backward rapidity.

Furthermore, the measurements are compatible with the 5 TeV results [18].

4.3 Forward-Backward production ratio

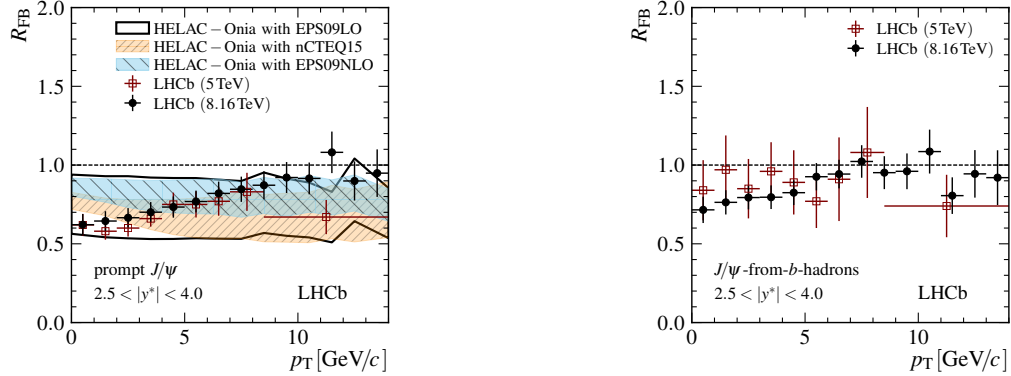


Figure 9: Forward-to-backward ratios, R_{FB} , integrated over the common rapidity range $2.5 < |y^*| < 4.0$ as a function of p_T for (left) prompt J/ψ and (right) J/ψ -from- b -hadrons.

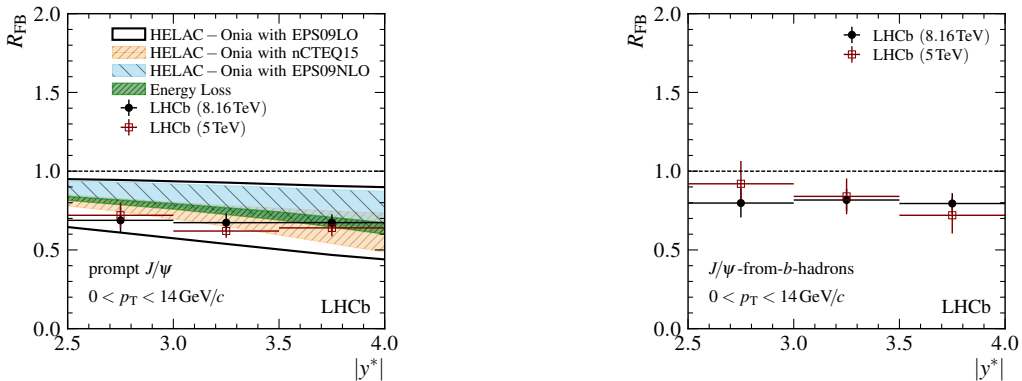


Figure 10: Forward-to-backward ratios, R_{FB} , integrated over p_T in the range $0 < p_T < 14$ GeV/c as a function of $|y^*|$ for (left) prompt J/ψ and (right) J/ψ -from- b -hadrons.

For prompt J/ψ and nonprompt J/ψ , we also measure the forward to backward production ratio

$R_{\text{FB}}(p_{\text{T}}, y^*)$. The measurements as a function of p_{T} or y^* are shown in Fig. 9 and Fig. 10 in comparison with those in $p\text{Pb}$ collisions at $\sqrt{s}=5$ TeV [18] and theoretical calculations.

The measurements of $R_{\text{FB}}(p_{\text{T}}, y^*)$ at $\sqrt{s}=5$ TeV and at $\sqrt{s}=8.16$ TeV are found to be in agreement. The experimental results agree with the predictions based on HELAC-onia with different nPDFs within uncertainties for prompt J/ψ . The coherent energy loss calculation is compared with the rapidity dependence of the experimental data points. The slope is slightly differs from the one observed with the experimental data points.

5 Summary

LHCb has collected large data samples in proton-lead collisions. A new measurement of prompt D^0 production in $p\text{Pb}$ and $\text{Pb}p$ collisions at $\sqrt{s}=5$ TeV shows strong cold nuclear matter effects that can be described by calculations using nPDFs, CGC framework. The first result for J/ψ production in $p\text{Pb}$ and $\text{Pb}p$ collisions at $\sqrt{s}=8.16$ TeV at LHC has been measured. Prompt and non-prompt J/ψ production results show clear suppression and confirm the findings at $\sqrt{s}=5$ TeV [18] with higher precision. Theoretical calculations for the nuclear modification factor based on collinear factorisation with different nuclear parton distribution functions, coherent energy loss as well as the color glass condensate approach calculation can account for the majority of the observed dependencies for prompt J/ψ . Calculations from the FONLL coupled with the EPS09 nPDF set can overall describe the data points within uncertainties for the non-prompt J/ψ .

References

- [1] R. Aaij *et al.* [LHCb Collaboration], Study of prompt D^0 meson production in $p\text{Pb}$ collisions at $\sqrt{s} = 5$ TeV, Accepted by JHEP, [arXiv:1707.02750].
- [2] R. Aaij *et al.* [LHCb Collaboration], Prompt and nonprompt J/ψ production and nuclear modification in $p\text{Pb}$ collisions at $\sqrt{s} = 8.16$ TeV, Phys. Lett. B **774** (2017) 159-178, [arXiv:1706.07122].
- [3] H.Fujii, F. Gelis, and R. Venugopalan, Quark pair production in high energy pA collisions: General features, Nucl. Phys. A **780**, 146 (2006) [arXiv:0603099 [hep-ph]].
- [4] D. Kharzeev and K. Tuchin, Signatures of the color glass condensate in J/ψ production off nuclear targets, Nucl. Phys. A **770**, 40 (2006) [arXiv:0510358 [hep-ph]].
- [5] F. Arleo and S.Peigne, Heavy-quarkonium suppression in pA collisions from parton energy loss in cold QCD matter, JHEP **03**, (2013) 122 [arXiv:1212.0434].
- [6] A. A. Alves Jr. *et al.* [LHCb Collaboration], The LHCb detector at the LHC, JINST 3 (2012) S08005.
- [7] R. Aaij *et al.* [LHCb Collaboration], LHCb detector performance, Int. J. Mod. Phys. A **30** (2015) 1530022, [arXiv:1412.6352].
- [8] K. J. Eskola, H. Paukkunen, and C. A. Salgado, EPS09: A New generation of NLO and LO Nuclear Parton Distribution Functions, JHEP **04**, (2009) 065, [arXiv:0902.4154].
- [9] K. Kovarik *et al.*, nCTEQ15 - Global analysis of nuclear parton distributions with uncertainties in the CTEQ framework, Phys. Rev. D **93** (2016), 085037, [arXiv:1509.00792].
- [10] J.-P. Lansberg and H.-S. Shao, Towards an automated tool to evaluate the impact of the nuclear modification of the gluon density on quarkonium, D and B meson production in proton-nucleus collisions, Eur. Phys. J. C **77** (2017), 1, [arXiv:1610.05382].
- [11] H.-S. Shao, HELAC-Onia 2.0: an upgraded matrix-element and event generator for heavy quarkonium physics, Comput. Phys. Commun. **198** (2016) 238, [arXiv:1507.03435].

- [12] H.-S. Shao, HELAC-Onia: An automatic matrix element generator for heavy quarkonium physics, *Comput. Phys. Commun.* **184** (2013) 2562, [arXiv:1212.5293].
- [13] M. Cacciari, M. Greco, and P. Nason, The p_T spectrum in heavy-flavour hadroproduction, *JHEP* **05** (1998) 007, [arXiv:hep-ph/9803400].
- [14] M. Cacciari, S. Frixione, and P. Nason, The p_T spectrum in heavy-flavour hadroproduction, *JHEP* **03** (2001) 006, [arXiv:hep-ph/0102134].
- [15] B. Ducloué, T. Lappi, and H. Mäntysaari, Forward J/ψ production in proton-nucleus collisions at high energy, *Phys. Rev. D* **91** (2015) 114005, [arXiv:1503.02789].
- [16] B. Ducloué, T. Lappi, and H. Mäntysaari, Forward J/ψ production at high energy: centrality dependence and mean transverse momentum, *Phys. Rev. D* **94** (2016) 074031, [arXiv:1605.05680].
- [17] R. Aaij *et al.* [LHCb Collaboration], Production of J/ψ and Υ mesons in pp collisions at $\sqrt{s} = 8 \text{ TeV}$, *JHEP* **06** (2013) 064, [arXiv:1304.6977].
- [18] R. Aaij *et al.* [LHCb Collaboration], Study of J/ψ production and cold nuclear matter effects in $p\text{Pb}$ collisions at $\sqrt{s} = 5 \text{ TeV}$, *JHEP* **02** (2014) 072, [arXiv:1308.6729].